Hindawi
Advances in Civil Engineering
Volume 2022, Article ID 4456439, 16 pages
https://doi.org/10.1155/2022/4456439

Research Article

Structural Damage Localization in Plates Using Global and Local Modal Strain Energy Method

Thanh-Cao Le,[1,2,3] **Duc-Duy Ho**,[1,2] **Chi-Thien Nguyen**,[1,2] **and Thanh-Canh Huynh**[4,5]

[1]*Faculty of Civil Engineering, Ho Chi Minh City University of Technology (HCMUT), Ho Chi Minh City 700000, Vietnam*
[2]*Vietnam National University Ho Chi Minh City, Ho Chi Minh City 700000, Vietnam*
[3]*Faculty of Civil Engineering, Nha Trang University, Nha Trang 57100, Vietnam*
[4]*Faculty of Civil Engineering, Duy Tan University, Da Nang City 550000, Vietnam*
[5]*Center for Construction, Mechanics, and Materials, Institute of Research and Development, Duy Tan University, Da Nang City 550000, Vietnam*

Correspondence should be addressed to Duc-Duy Ho; hoducduy@hcmut.edu.vn

Received 12 December 2021; Accepted 26 April 2022; Published 18 May 2022

Academic Editor: Qian Chen

This paper presents an improvement to the modal strain energy (MSE) method for identifying structural damages in plate-type structures. A two-step MSE-based damage localization procedure, including a global step and a local step, is newly proposed to enhance the accuracy of detecting the location of structural damage. Firstly, the global step uses the mode shape data on the whole plate to locate the potentially damaged areas. Then, MSE is applied with a more dense mesh size on these local areas to detect damage in more detail. The proposed procedure's feasibility is verified by analyzing an aluminum plate with various damaged scenarios. This study uses finite element analysis to acquire the plate's natural frequencies and mode shapes in intact and damaged states. A set of two damage detection capacity indicators are also newly presented to evaluate the precision of the proposed procedure. The diagnostic results demonstrate that the proposed approach uses less modal data than the original MSE method and accurately identifies the damage's locations in the plates with various edge conditions. Moreover, the combination of three first mode shapes and a damage threshold of 40% of the maximum normalized damage index gives the best results of damage localization.

1. Introduction

During the last few decades, structural health monitoring (SHM) has played an essential role in civil structures' safety and sustainable performance. Many researchers have focused attention on non-destructive detection techniques for identifying structural damages, particularly techniques based on structural vibration responses. Among these methods, the curvature and modal strain energy (MSE) methods emerged as effective approaches to identify the structural damage in beam and plate structures. Yang [1] proposed an improved curvature technique using the change of the mode shape information to detect damage in bridge structure. The suggested approach's effectiveness has been demonstrated using a numerical and experimental model of an intact and damaged steel plate subjected to impact forces. As predicted by the proposed theory, the change in mode shape exhibits a strong correlation with the embedded damage. Zhong [2] presented a method using two-dimensional mode shape curvatures for identifying damage in plate-like structures. Numerous numerical simulations and experimental models on a steel plate demonstrated that the modified method works well for detecting damage. Furthermore, this approach only requires the first few mode shapes of the intact and damaged plate. It even needs modal information of the damaged state if the gapped smoothing technique is used.

Besides, damage detection approaches based on MSE changes have been also widely used. These methods use the fractional MSE change of undamaged and damaged states of

the target structure to identify the damages. The MSE value can be directly derived from 1D mode shape curvature in beams and 2D mode shape curvature in plates. Hence, the MSE-based method is considered a particular case of the mode shape curvature-based method for beam or plate structures. Compared to the mode shape curvature-based method, the MSE-based method is more sensitive to damage because it considers curvature change in more directions. In other words, the mode shape curvature-based method is effective in beam-type structures; meanwhile the MSE-based method works well for both beam-type and plate-type structures.

Shi [3] proposed the change in MSE as a practical methodology for damage detection. A numerical simulation and an experimental test were conducted on portal steel frame structures to derive the sensitivity of the MSE concerning damage. The results showed that the MSE method could locate multiple damages, but it was quite sensitive to noise. Alvandi [4] introduced the MSE method to estimate damage in a simple supported beam with various damage ratios. The results proved that among vibration properties (e.g., mode shape, flexibility, and flexibility curvature), the MSE change was the most reliable and stable indicator to detect damage regarding noisy signals. However, the damage identification ability depended on the used threshold level.

The following typical studies developed the MSE procedure to detect the position of structural damages. Stubbs [5] developed a global MSE theory for beam structures using mode shapes and elemental stiffness matrices. Modal data of intact and damaged states extracted from a bridge in New Mexico were fed into the damage detection algorithm. Analysis results indicated that this methodology could locate the damages accurately. Cornwell [6] applied the MSE method for localising structural damage in plate-type structures, using only some mode shapes data in pre-damage and post-damage states. Unlike the natural frequency-based methods, the MSE method could detect areas with stiffness reduction as small as 10%. In addition, this method was validated for its effectiveness in both simulated and experimental data.

Shi [3] introduced a damage identification technique based on the MSE change in truss and 2D frame structures. Basically, the MSE value of undamaged elements changed a small amount compared to damaged elements. Therefore, the MSE change ratio (MSECR) indicator was very significant to locate the damages. Besides, the calculation of MSECR required no prior information about the structure except for the structure's stiffness and mode shape matrix. This method was proved to identify multiple structural damages accurately in case of noise or lack of measured mode if using combined modes.

Shih [7] proposed a multicriteria technique combining modal flexibility and the MSE method for assessing multiple damages in beam and plate structures. From the modal analysis results, algorithms obtained flexibility and MSE changes of intact and damaged structures to assess the structural health status. It was described that the proposed approach provides sensitivity, reliability, and accuracy on multiple damage localization. Le [8] presented the MSE approach for detecting damage in plates, considering various edge conditions. The central difference method was employed to calculate the second-order derivatives in the MSE formula. This approximation technique only required the transverse displacement components at grid nodes and virtual boundary points. A damage index was established to determine the position and size of faults in plate structures. According to the results obtained, the suggested approach could correctly identify fractures in the plate structure under various edge conditions.

Recently, several two-step approaches combining the MSE method and optimization algorithms were presented to detect the positions and estimate the severity of structural damages. Seyedpoor [9] proposed a two-step procedure to determine the multiple damages in terms of their locations and extents. The first step using an MSE-based index was to determine the damage's location. Particle swarm optimization was employed to estimate the damage severity in the next step. For steel 3-D frame structures, Cha [10] proposed a damage identification method incorporating the MSE approach and hybrid multi-objective optimization. The technique could detect structural damages of minor severity. To identify the damage position and its extent in laminated composite plates, Vo-Duy [11] integrated the MSE method with an advanced differential evolution algorithm. The impact of data noise on damage detection accuracy was also examined. Torkzadeh [12] developed a two-step strategy using improved artificial neural networks combining curvature-moment derivatives to detect cracks in flexural plates. The multiple-damage location assurance criterion index based on the frequency change vector of structures was evaluated using an adequately trained cascade feed-forward neural networks as a surrogate model. The results showed that the Bat algorithm engaged by an appropriate artificial neural networks model as a surrogate of the direct finite element model significantly reduces the computational time of model updating during the damage extent detection process. Kaveh [13] used the MSE-based index and the cyclical parthenogenesis procedure to identify the impairment of the parts for the 2D frame structures. Dinh-Cong [14] proposed a two-step procedure for detecting plate damage, combining the normalized damage index based on MSE change and the Jaya heuristics. Two objective functions were formed using the modal flexibility variation and the mode shape change. Khatir [15] suggested a damage detection approach combining the normalized damage index based on MSE change and an optimization technique based on teaching-learning to determine the position and magnitude of impairments in beam structures. Zhao [16] developed a damage localization technique based on the MSE change ratio method and the MSE dissipation ratio method to detect the potential damage positions. Then, the evidence theory is used to combine these results and detect precisely the structural damage locations.

Next, Fathnejat [17] suggested a surrogate model of the structure in a two-step procedure for detecting structural damage in space truss structures. Three popular optimization algorithms with the objective function based on the root mean square deviation of the modal property change vector

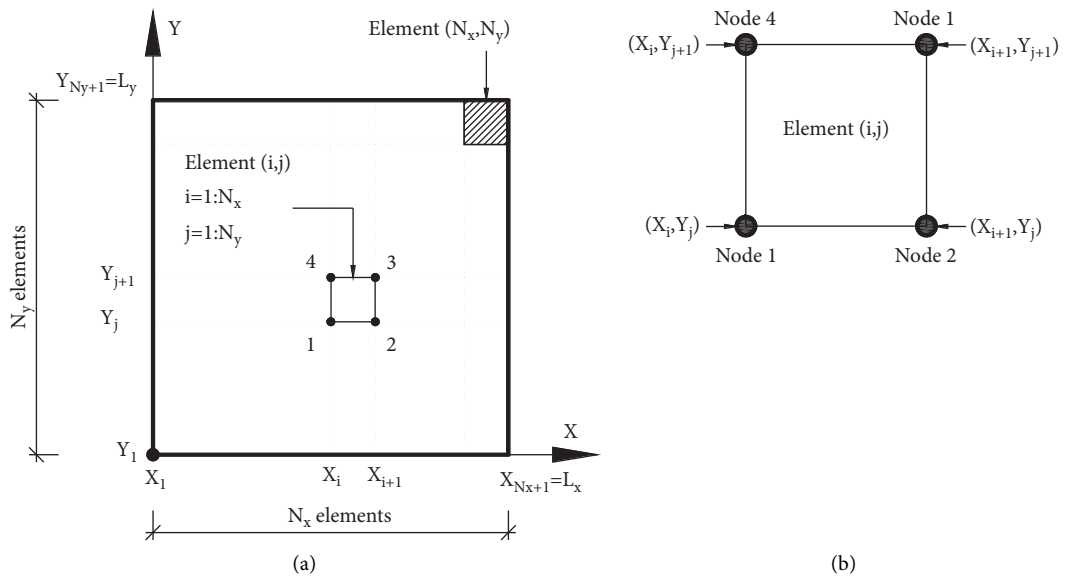

Figure 1: Illustration of a rectangular plate: (a) whole plate and (b) element (i, j).

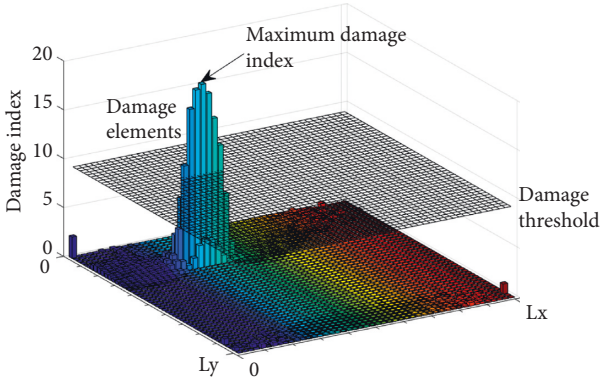

Figure 2: Damage index chart.

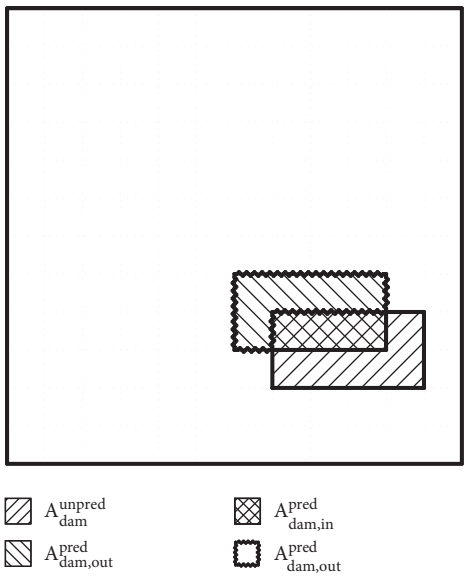

Figure 3: Illustration of the parameters to determine the detection capacity indicators.

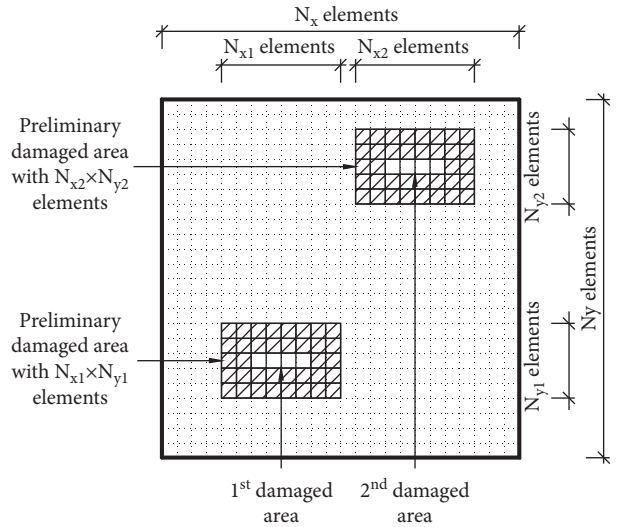

Figure 4: Illustration of the preliminary damaged area.

(particle swarm optimization, bat algorithm, and colliding bodies) were examined for the ability to estimate damage extent. The results showed that the combination of particle swarm optimization and the mean normalized modal strain energy gives the best accuracy of damage extent estimation. Nick [18] proposed a two-step damage detection procedure to identify both positions and extents of damages in steel girder structures. Firstly, a damage index based on MSE change was calculated for the three first flexural modes to determine the damage position. In the second step, damage indexes were used as input data to train the artificial neural networks to predict the severity of structural damages. Kaveh [19] presented a Graph-based Adaptive Threshold (GAT) to identify damaged elements not be detected by the basic MSEBI in the first step. GAT was a modest anomaly detection approach that uses ideas from graph theory and

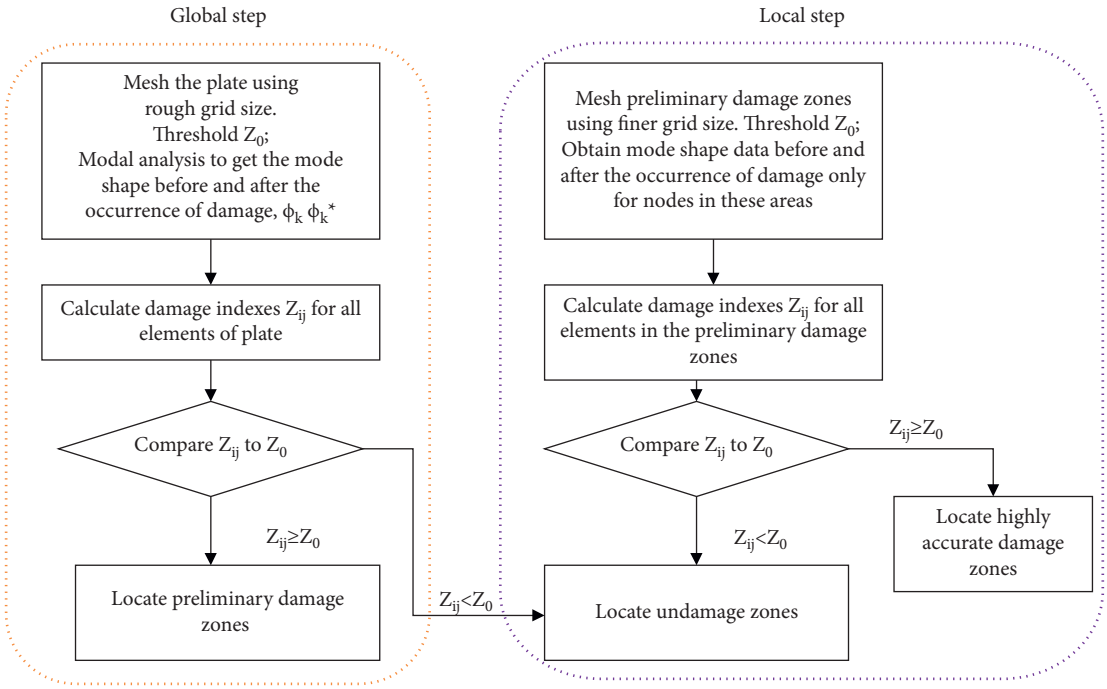

Figure 5: The proposed two-step MSE-based damage localization procedure.

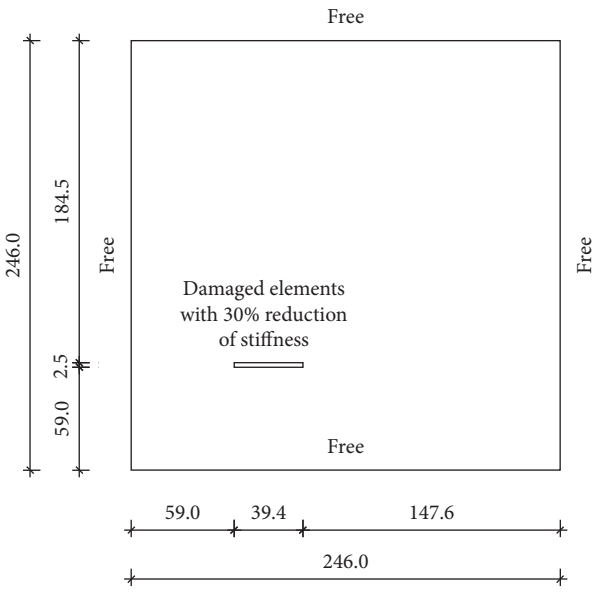

Figure 6: Free boundary square plate with a crack.

MSE. In the second step, an improved version of the Water Strider Algorithm was suggested to identify damages in conditions of insufficient modal data and input data noise. Sadeghi [20] proposed a new technique for damage identification in steel-concrete composite beams based on modal strain energy change and general regression neural network (GRNN). Three modal strain energy change ratios caused by the elemental stiffness reduction in the steel, concrete, and shear connection layers were calculated as damage indices to determine the structural damage in the composite layers. The low dimensional data were employed as the input for the GRNN in various damage scenarios. The results indicated that the suggested procedure can effectively identify minor damage in the composite beam using a few modes. Fan [21] proposed an improved damage index, called Modified Index of Cross-model MSE, constructed on cross-model MSE to locate the damaged elements. Then simultaneous optimization was introduced to estimate the damaged extent of elements. The two-step procedure eliminates the requirement to calculate the modal parameter sensitivity and reanalyze the characteristic equation. Moreover, this method made the diagnostic algorithm converge faster and ensures the precision of damage identification results. Belhadj [22] proposed a two-stage optimization procedure based on the modal strain energy and an Efficient Accelerated Particle Swarm Optimization algorithm (EAPSO) to detect the position and quantify the extent of damage in plate-type structures. First, a new damage index was calculated using the modal strain energy and the statistical hypothesis analysis technique to locate potential damaged sites. Next, the EAPSO with the objective function based on flexibility matrix changes was used to estimate the extent of damaged elements localized from the first stage.

The MSE method has been deployed on the whole structure for the previous studies to search the potentially damaged areas. However, this global procedure requires complete mode shape data on the entire plate to guarantee the accuracy of the damage detection results. Therefore, it is time-consuming and complex in practice because of the difficulties of acquiring mode shape data on the whole structure with dense measured points. Furthermore, plate-type structures such as floor and wall components are essential individual elements in civil structures. Structural damages (e.g., crack and fault) under loads and

Table 1: Variations of natural frequencies (Hz) according to the mesh sizes of the intact plate.

Mode	Mesh size					
	20%	10%	5%	4%	2%	1%
1	106.1	107.5	107.0	106.9	106.8	106.9
2	163.5	158.5	157.1	157.0	156.5	156.7
3	213.6	202.3	199.5	199.1	198.8	198.6

Table 2: Natural frequency convergence (%) in comparison to the plate dimension's mesh size of 1%.

Mode	Mesh size				
	20%	10%	5%	4%	2%
1	0.8	0.6	0.1	0.1	0.0
2	4.4	1.1	0.3	0.2	0.1
3	7.6	1.9	0.5	0.3	0.1

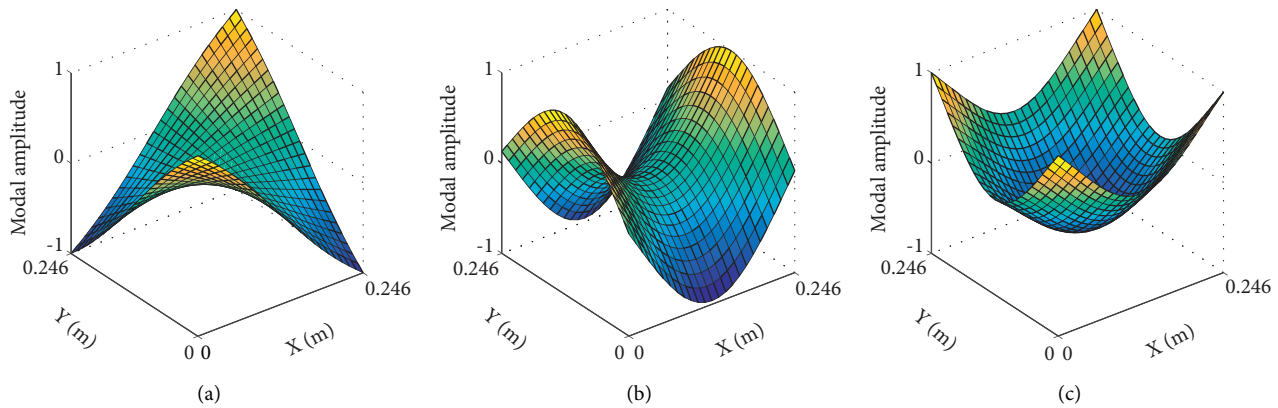

Figure 7: The first three flexural mode shapes of the free intact plate: (a) Mode 1, (b) Mode 2, and (c) Mode 3.

Table 3: Comparison of natural frequencies.

Mode	Natural frequency (Hz)				Difference (%)		
	This study	Hu [23]	Blevins [24]	SAP2000	Hu [23]	Blevins [24]	SAP2000
1	107.0	106.0	109.8	107.4	0.9	2.6	0.4
2	157.1	157.0	161.0	156.7	0.1	2.5	0.3
3	199.5	196.0	198.8	198.6	1.7	0.3	0.5

environmental effects weaken the structural strength of individual elements and the whole system. So these damages must be identified and controlled to ensure structural stability and operation of a system. No study has been done on structural damage identification in plate structure at the local level using the MSE-based damage indexes so far. Therefore, it is essential to develop a global and local MSE-based damage identification procedure for plate structure using as little mode shape data as possible.

The main objective of this study is to develop the MSE-based damage identification theory for plate-type structures that use fewer mode shape data than the global MSE method but still ensure the accuracy of the damage localization results. The feasibility of the presented procedure is verified by investigating plates with various damaged scenarios. Finite element analyses are performed on aluminum plates to acquire the data of mode shapes in intact and damaged

Table 4: Change of natural frequencies due to damage.

Mode	Intact state (Hz)	Damaged state (Hz)	Change (%)
1	107.0	106.9	0.12
2	157.1	156.9	0.12
3	199.5	199.2	0.13

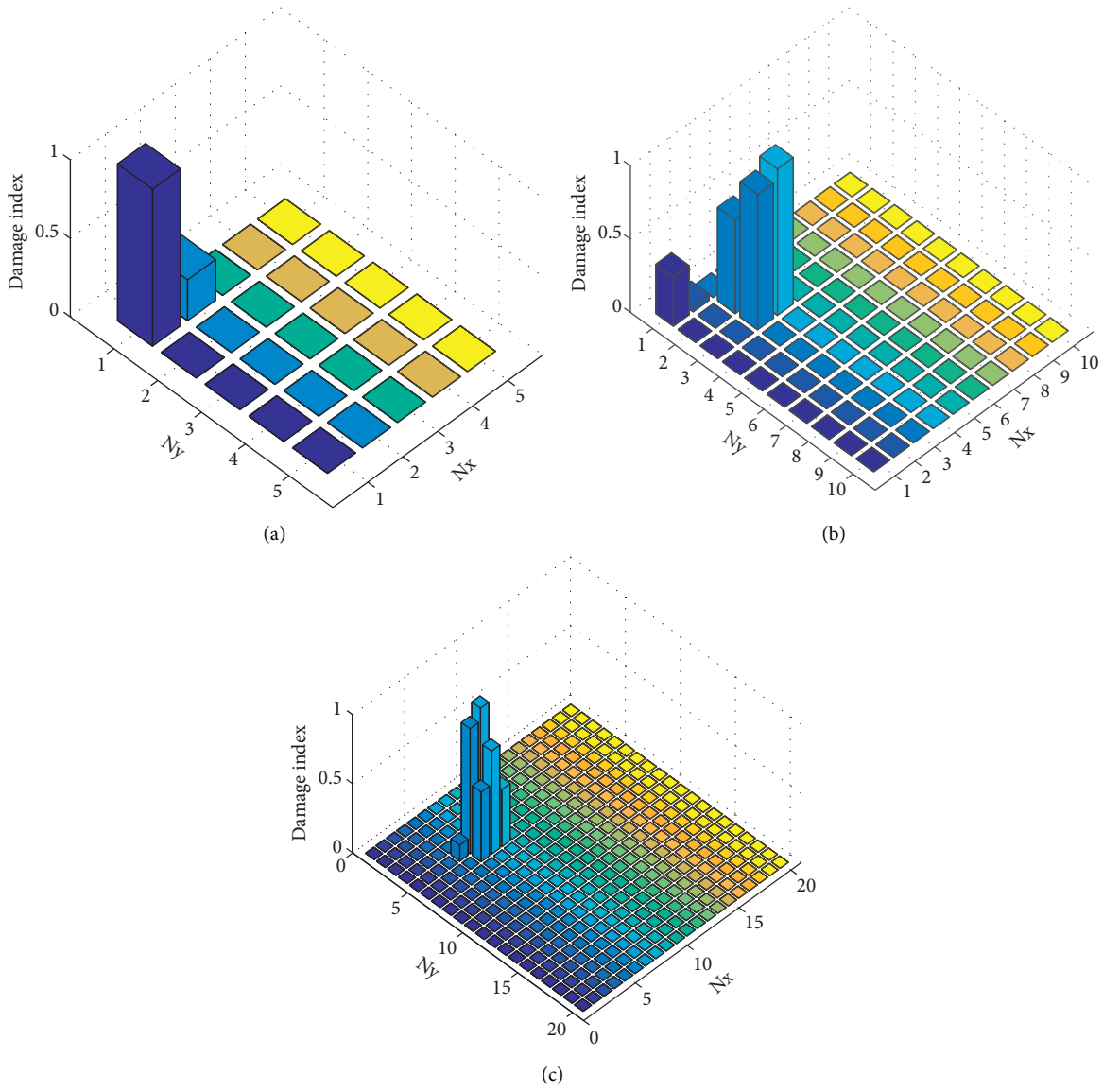

Figure 8: Truncated damage index charts using damage threshold 40% $Z_{ij}^{\max}$: (a) Mesh 20%, (b) Mesh 10%, and (c) Mesh 5%.

Table 5: Damage capacity indicators (%) for global MSE procedure.

Mesh size	Indicator	Damage threshold					
		20%	30%	40%	50%	60%	70%
20%	A (%)	100	100	100	0	0	0
	B (%)	9,900	7,400	7,400	5,000	2,500	2,500
10%	A (%)	100	100	100	100	100	100
	B (%)	6,775	4,275	3,650	3,025	4,275	1,775
5%	A (%)	100	100	100	75	75	75
	B (%)	2,088	994	994	863	863	550

states. Moreover, two detection capacity indicators are also newly presented to evaluate the capacity of damage localization for the damaged zone, undamaged zone, and whole plate, respectively. Finally, the effectiveness of the local process on the precision of damage detection results compared to the global MSE method is also investigated. According to the analytical results, despite employing fewer mode shape data, the suggested technique accurately identifies damage areas in plate-type structures. The results from this study can be applied to various engineering fields, such as civil engineering, mechanical engineering, and aerospace engineering.

2. Modal Strain Energy-based Damage Localization Method

2.1. Theory of MSE-based Damage Localization Method. The primary input data for the MSE method are mode shape features extracted from vibration analysis. The mode shapes of plate structures are characterized by the 2D curvatures. For example, a rectangular plate is meshed into four-node elements to analyze the modal vibration, as depicted in Figure 1(a). N_x and N_y represent the number of elements in x and y axes; For a particular (i, j) element, its node indexes and coordinates are shown in Figure 1(b).

The partial MSE value of the subregion (i, j) for the kth mode shape, $\phi_k(x, y)$, is calculated as follows [23]:

$$MSE_{k,ij} = \frac{B_{ij}}{2}\int_{x_i}^{x_{i+1}}\int_{y_j}^{y_{j+1}}\left(\frac{\partial^2\phi_k}{\partial^2 x}\right)^2 + \left(\frac{\partial^2\phi_k}{\partial^2 y}\right)^2 + 2\nu\left(\frac{\partial^2\phi_k}{\partial^2 x}\right)\left(\frac{\partial^2\phi_k}{\partial^2 y}\right) + 2(1-\nu)\left(\frac{\partial^2\phi_k}{\partial x\,\partial y}\right)^2 \mathrm{d}x\mathrm{d}y, \quad (1)$$

where B_{ij} is the bending stiffness of the subregion (i, j); ν is the Poisson coefficient of the plate's material.

The total MSE value of the whole plate is the sum of all partial MSE values:

$$MSE_k = \sum_{i=1}^{N_x}\sum_{j=1}^{N_y} MSE_{k,ij}. \quad (2)$$

The kth mode shape of the damaged state is defined as $\phi_k^*(x, y)$. Similarly, $MSE_{k,ij}^*$ and MSE_k^* of the damaged state, denoted by symbol "*", are calculated as (1 and 2) The fractional MSE of the sub-region (i, j) is given by:

$$F_{k,ij} = \frac{MSE_{k,ij}}{MSE_k}, \quad (3)$$

$$F_{k,ij}^* = \frac{MSE_{k,ij}^*}{MSE_k^*}. \quad (4)$$

The damage index for the element (i, j) considering m modes is defined as:

$$\beta_{ij} = \frac{\sum_{k=1}^{m} F_{k,ij}^*}{\sum_{k=1}^{m} F_{k,ij}}. \quad (5)$$

Finally, the damage index is normalized using the mean value $\overline{\beta}$ and standard deviation σ of the damage indices:

$$Z_{ij} = \frac{\beta_{ij} - \overline{\beta}}{\sigma}, \quad (6)$$

Z_{ij} is used as an indicator for detecting the occurrence and the location of potential damages in the plate. The second-order derivatives in (1), such as $\partial^2\phi_k/\partial^2 x, \partial^2\phi_k/\partial^2 y$, $\partial^2\phi_k/\partial x\,\partial y$, can be approximated using The Central Difference Method [6].

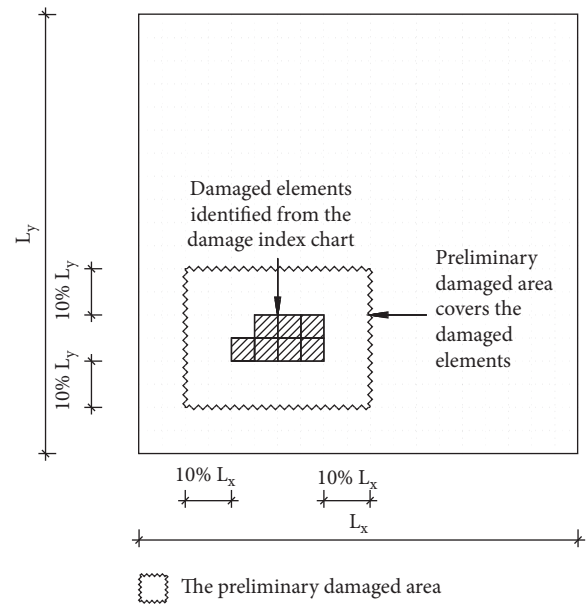

Figure 9: Preliminary damaged area detected from the global procedure.

2.2. Global MSE-based Damage Localization Procedure. The global MSE-based damage localization procedure, including seven steps, was presented by Le [8]. In the first step, the mode shape data is obtained by performing modal analysis on the free vibration of the target plate. This study analyzes the plate using the finite element method to obtain vibration data for both undamaged and damaged states. In the second step, the mode shape curvatures are determined. The Central Difference Method [8] utilises the virtual boundaries and nodal transverse displacement values to calculate the second-order derivatives. In the third step, the undamaged and damaged states' modal strain energies are calculated by (3 and 4), respectively. (5) is used in the fifth stage to compute the damage index. (6) is then used to compute the normalized damage index. As illustrated in Figure 2 [8], the normalized damage index chart is combined with a damage threshold of Z_o, to locate the potentially damaged areas in the sixth step. Finally, a set of two detection capacity indicators (i.e., A and B) is newly proposed to assess the capacity of damage localization.

The accuracy of the damaged area localization (indicator A) is determined as follows:

$$A = \frac{A_{\mathrm{dam,in}}^{\mathrm{pred}}}{A_{\mathrm{dam}}^{\mathrm{real}}}, \quad (7)$$

where $A_{\mathrm{dam,in}}^{\mathrm{pred}}$ is the predicted damaged area obtained from the damage index chart after truncation that stays in the actual damaged area of $A_{\mathrm{dam}}^{\mathrm{real}}$. The indicator of A varies from 0 to 1. In case A equals 0, the procedure cannot identify any damaged area. Otherwise, if A equals 1, it corresponds to the ability to locate all damaged areas.

The previous studies usually only focused on assessing the accuracy of localization results for damaged areas. However, in some cases, the damage localization procedure

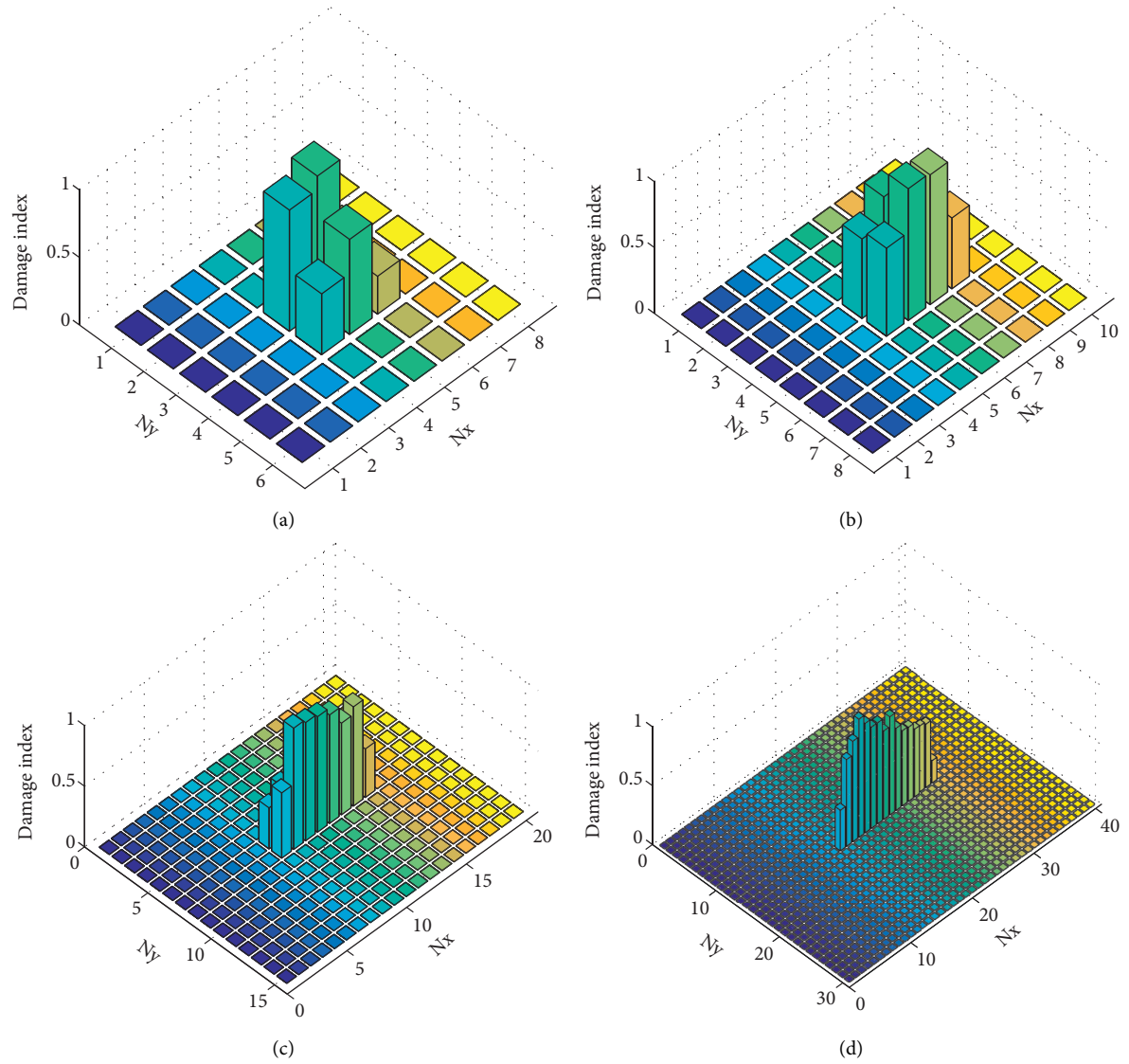

FIGURE 10: Truncated damage index charts of the preliminary damaged area using a damage threshold of 40% $Z_{ij}^{\max}$: (a) Mesh 5%, (b) Mesh 4%, (c) Mesh 2%, and (c) Mesh 1%.

misidentified damaged areas in the actual undamaged areas. Therefore, an indicator B is newly presented to assess the accuracy of undamaged area localization as follows

$$B = \frac{A_{\text{dam,out}}^{\text{pred}}}{A_{\text{dam}}^{\text{real}}}, \tag{8}$$

where $A_{\text{dam,out}}^{\text{pred}}$ is the misidentified damaged area obtained from the damage index chart after truncation. The smaller the B indicator value is, the better the undamaged area identification capability of the procedure is.

The parameters mentioned above are illustrated in Figure 3. For more details,

$$\begin{aligned} A_{\text{dam}}^{\text{real}} &= A_{\text{dam}}^{\text{unpred}} + A_{\text{dam,in}}^{\text{pred}}, \\ A_{\text{dam,out}}^{\text{pred}} &= A_{\text{dam}}^{\text{pred}} - A_{\text{dam,in}}^{\text{pred}}. \end{aligned} \tag{9}$$

2.3. Local MSE-based Damage Localization Procedure. The critical disadvantage of the global MSE-based damage localization procedure is the requirement of mode shape data on the whole plate. Moreover, a dense element mesh and many mode shape data are essential for highly accurate damage detection results. These drawbacks make the global procedure infeasible to deploy in practice. Therefore, the local MSE-based damage localization procedure is newly proposed to increase the feasibility of the MSE method. In the first step, the global MSE-based damage localization procedure is performed on the whole plate with a significant element mesh size to locate preliminary damaged areas. With the use of a significant element mesh size, the exact damage areas can not be determined. Therefore, the primary purpose of this step is only to locate the site where damage can occur, as illustrated in Figure 4. In the second step, the local MSE-based damage localization procedure is

Table 6: Damage capacity indicators (%) for local MSE procedure.

Mesh size	Indicator	Damage threshold					
		20%	30%	40%	50%	60%	70%
5%	A (%)	100	100	75	75	75	50
	B (%)	1,150	994	863	863	706	419
4%	A (%)	100	100	100	100	100	75
	B (%)	700	700	700	700	700	525
2%	A (%)	100	100	100	100	88	75
	B (%)	450	300	275	225	138	100
1%	A (%)	100	100	100	94	88	63
	B (%)	150	25	0	0	0	0

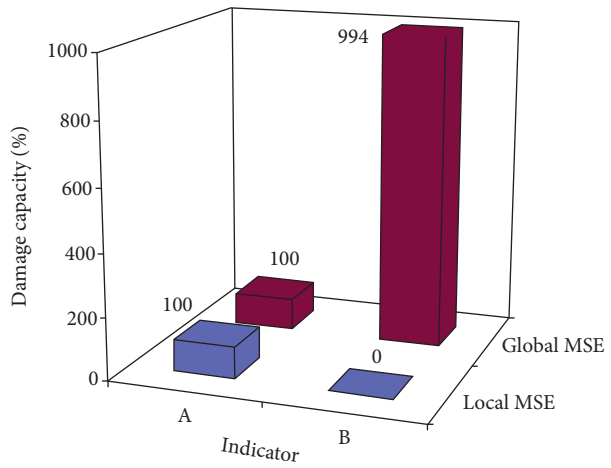

Figure 11: Damage capacity indicators for global and local procedures, using damage threshold 40% $Z_{ij}^{\max}$.

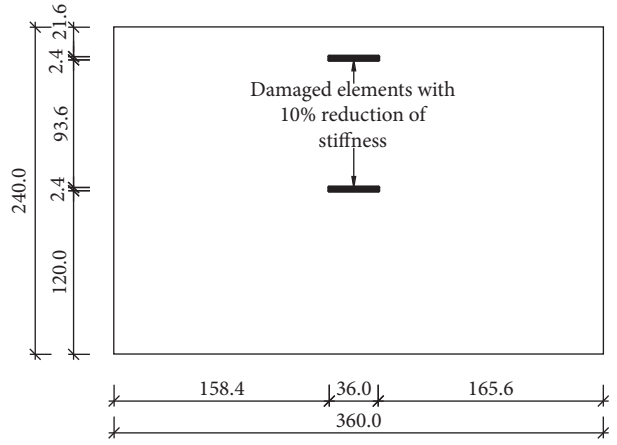

Figure 12: Rectangular plate, four fixed boundaries, with two cracks.

performed separately for each localized damaged area in the first step with a minor element mesh size to determine in more detail the damaged areas. The local MSE-based localization procedure is similar to the global one. The essential advantage of the local procedure is that modal data only needs to be collected on a much smaller site than the whole plate. The local procedure does not need to modal reanalyze the plate, so the boundary conditions on the local damaged areas are not required. The two-step MSE-based damage localization procedure is presented in Figure 5.

3. Numerical Verification

In this study, a thin rectangular plate with the same geometrical and material properties as [23] is examined to evaluate the effectiveness of the suggested procedure. The

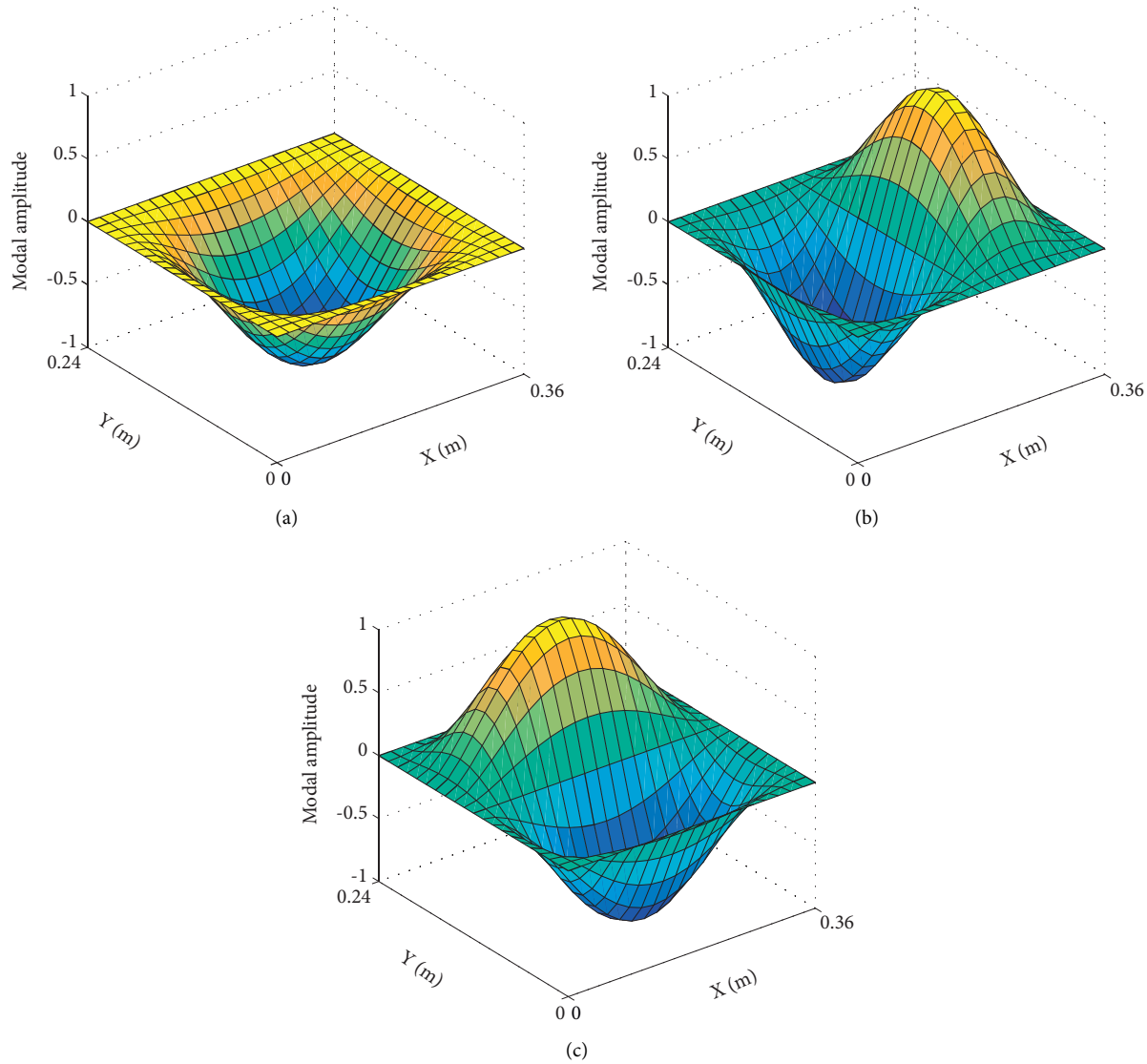

Figure 13: The first three flexural mode shapes of the undamaged plate, fixed boundary conditions: (a) Mode 1, (b) Mode 2, and (c) Mode 3.

plate size is 246×246×2 mm, as depicted in Figure 6. A damage scenario is assumed to be a surface crack with dimensions 39.4×2.5 m and a stiffness reduction of 30%. The location of the crack is also illustrated in Figure 6. The plate is made of aluminum with material properties: Elastic modulus E = 70 GPa, Poisson coefficient $\upsilon = 0.33$, and mass density $\rho = 2735$ kg/m3. The natural frequencies and mode shapes are determined using modal analysis with completely free boundary conditions.

Modal data are obtained by modelling and analyzing the plate using the finite-element method with four-node elements. The first flexural modes of the target plate at intact and damaged states extracted from the modal analysis are used as the input for the damage localization procedure. Through the global and local procedures, the output results are the occurrence, location, and detection capacity indicators. The damage identification capability of the proposed procedure is also analyzed for various element mesh sizes. The combination of the three first flexural modes shapes is used to calculate damage localization results. The damage threshold varying from 20% to 70% is also considered in this case.

3.1. Modal Analysis Results. A convergence study of natural frequency values acquired from FEM analysis is performed on various mesh sizes of the element. Mesh sizes of 1%, 2%, 4%, 5%, 10%, and 20% of the plate dimension were examined. Table 1 illustrates the effect of mesh size on the natural frequencies of the intact plate. Table 2 compares the convergence of natural frequencies of different mesh sizes to the mesh size 1% of the plate dimension. The convergence study shows that natural frequencies using the mesh size of 5% and of 1% are nearly identical. Therefore, the mesh size of 5% is sufficient to solve the modal analysis. Figure 7 presents the shapes of the first three flexural modes of the intact plate.

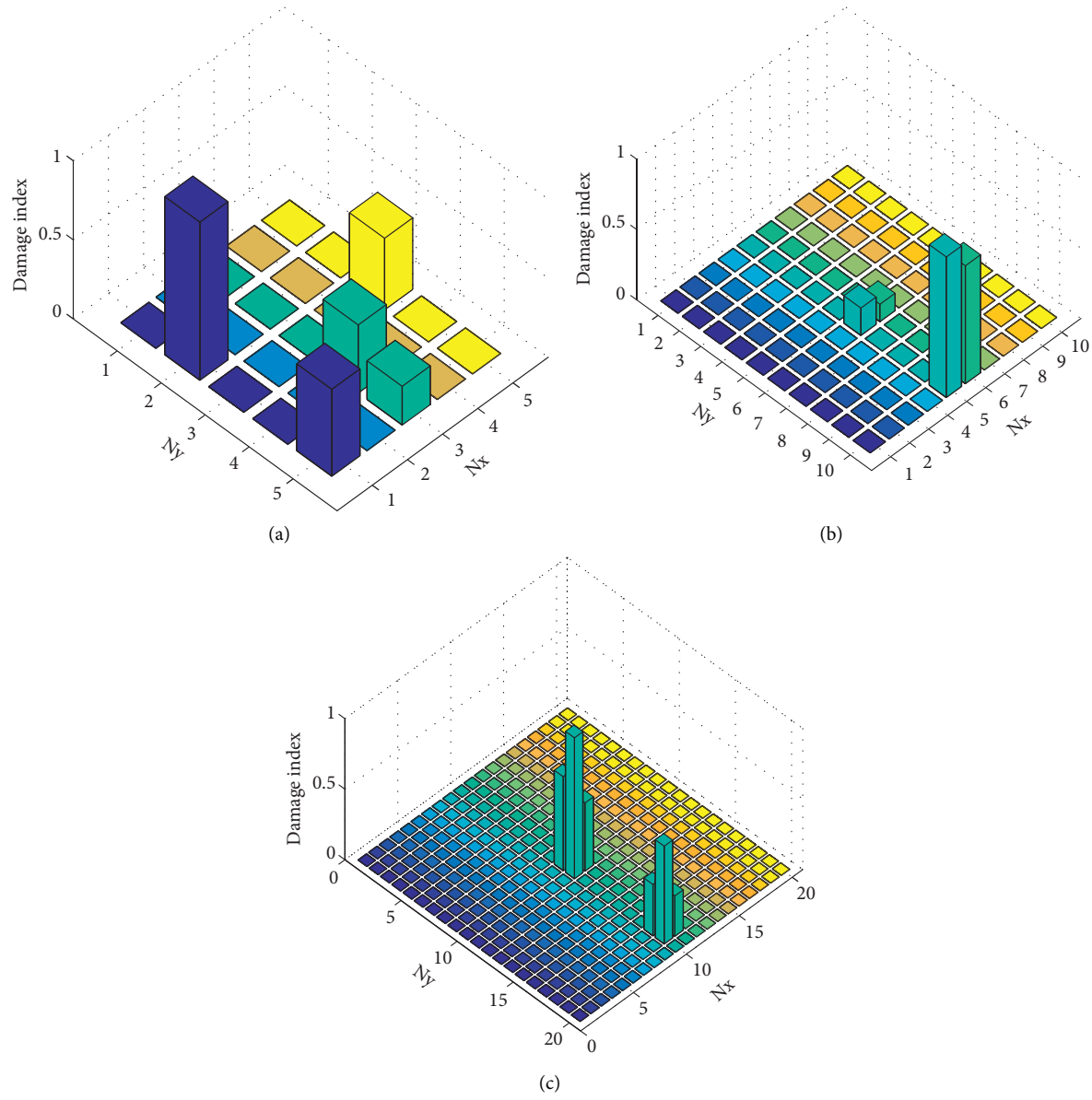

Figure 14: Truncated damage index charts using damage threshold 40% $Z_{ij}^{\max}$: (a) Mesh 20%, (b) Mesh 10%, and (c) Mesh 5%.

Table 7: Damage capacity indicators for extended verification using global MSE.

Mesh size	Indicator	Damage threshold					
		20%	30%	40%	50%	60%	70%
20%	A (%)	50	50	50	50	0	0
	B (%)	3,060,218	3,060,218	2,550,173	2,550,173	2,040,179	1,020,089
10%	A (%)	100	100	100	75	50	50
	B (%)	4,808,847	2,671,537	2,137,210	1,602,907	1,068,605	1,068,605
5%	A (%)	100	100	67	67	50	33
	B (%)	6,617,504	5,514,570	4,411,669	3,860,202	2,757,285	1,654,368

The natural frequencies obtained from FEA are also compared to the analytical ones suggested by Blevins [24], the experimental ones conducted by Hu [23], and the numerical ones obtained by SAP2000 software. As listed in Table 3, the natural frequencies' differences are inconsiderable, 0.1%-2.6%. This result proves that the modal analysis results in this study are credible. Table 4 shows that the natural frequencies decrease lightly by 0.12%-0.13% as the

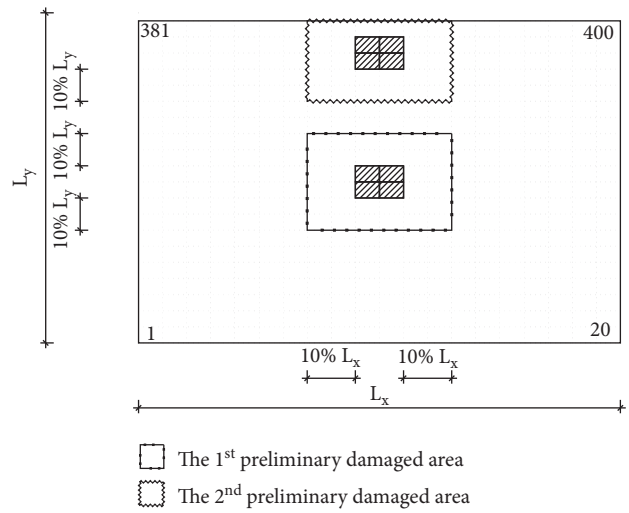

Figure 15: Two preliminary damaged areas detected from global MSE procedure.

damage occurs. The natural frequency changes are not sensitive to damage and are only used as an indicator to alarm the damage occurrence in the plate.

3.2. Global MSE-based Damage Localization Results. As mentioned above, if the damage index of an element is larger than the chosen damage threshold, the element is classified as a damaged one. Figure 8 shows the damage index chart after truncated by a damage threshold, $Z_0 = 40\% Z_{ij}^{\max}$ for 20%, 10%, and 5% element mesh, respectively. The figure shows that the damage can be localized as the local area. The damage detection results on the whole plate for various mesh sizes are summarized in Table 5.

Table 5 shows that the damage capacity indicators are dependent on the used damage threshold and element mesh size. If indicator A or indicator B is utilized separately, the assessment results are not objective. For example, in the case of mesh size 5%, indicator A, which represents the accuracy of the damaged zone, reaches a maximum value of 100%. However, this does not correspond to the maximum efficiency of damage localization. Indicator B decreases when the threshold increases using mesh sizes of 20%, 10%, and 5% for the same mesh size. For the same damage threshold, indicator B decreased considerably when the mesh size got smaller. However, indicator B is still significant in using a 5% mesh size for all the used thresholds. Therefore, the local MSE-based damage localization procedure needed to be investigated to improve the efficiency of damage localization.

3.3. Local MSE-based Damage Localization Results. After applying the global MSE-based damage detection procedure on the whole plate, the preliminary damaged areas are localized as a rectangle with a smaller size, as shown in Figure 9. From the areas of damage elements identified by the global procedure's damage index chart, the corresponding local damaged area is determined as a rectangular that is 20% larger in both x and y directions. The local MSE-based damage detection procedure is deployed on these areas with smaller element mesh sizes to evaluate the efficiency of identifying damaged elements. The element mesh sizes of 5%, 4%, 2%, and 1% are investigated. The damage localization results are shown in Figure 10 and summarized in Table 6. The results show that the local MSE-based damage localization procedure can identify the location of damage even with mesh 5% of the plate dimension.

As listed in Table 6, indicator B is decreased when the mesh size is decreased. As a result, the B value reaches 0%, corresponding to the exactly undamaged area detection when the element mesh size is 1%. The result also shows that indicator A gets the highest value when using the damage threshold of 40% with the same mesh size. Meanwhile, indicator B gets the smallest value when the damage used threshold is the largest. It should be noted that the damaged elements determined for the chart do not necessarily be the actual damaged elements. These elements can be called equivalent damaged elements because of the difference between the actual size of the damaged element and the mesh size of the element used to be detected.

From the above results, the appropriate parameters of the two-step procedure are proposed: For the global step, the element mesh size of approximately 5% is used to locate the initial areas of damage. Then, for the local step, smaller mesh size is used to locate more accurately damaged areas. Three first mode shapes are combined as input in both global and local steps to get more accurate and stable damage detection results. Moreover, a damage threshold of 40% $Z_{ij}^{\max}$ is used to eliminate some wrong damaged alarms. The preliminary damaged area is determined as a rectangular that is 20% larger in both x and y directions than the damaged regions detected from the global step's damage index chart. For example, the damaged area determined for the chart is rectangular with the size 9.84×4.92 mm. The plate size is 246×246 mm; as a result, the dimensions of the preliminary damaged area are 34.44×29.52 mm.

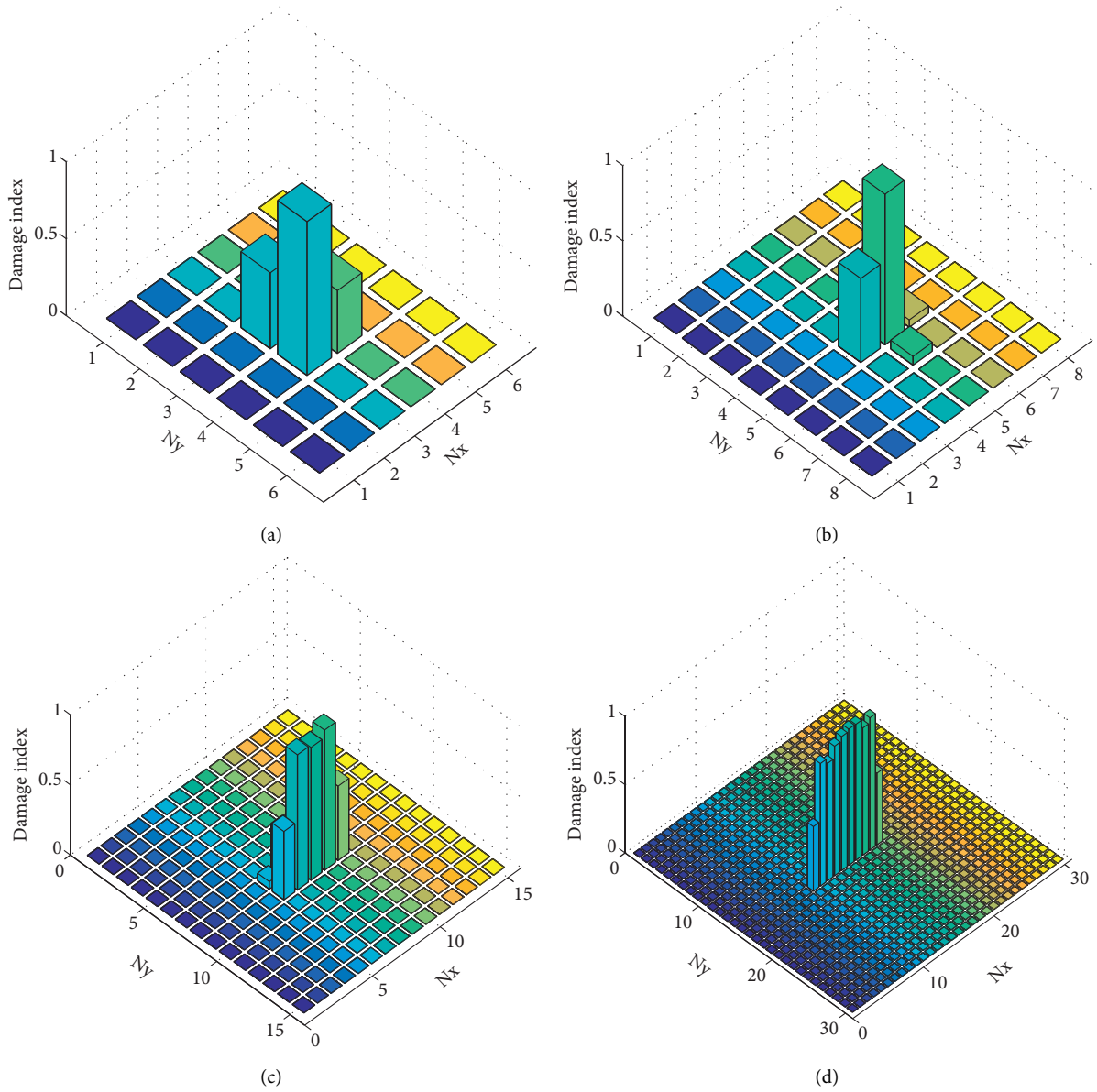

FIGURE 16: Truncated damage index charts of the first preliminary damaged area using damage threshold 40% $Z_{ij}^{\max}$: (a) Mesh 5%, (b) Mesh 4%, (c) Mesh 2%, and (d) Mesh 1%.

Figure 11 shows that the local MSE-based damage localization procedure significantly improves the accuracy of damage identification compared to the global one. For example, although the global procedure could detect the damaged area with a mesh size of 5%, it also misidentified the undamaged area with the rate of 994% for a damage threshold of 40% (Table 5). Meanwhile, using a mesh size of 1% on a much smaller preliminary damaged area than the whole plate, the local procedure eliminated all undamaged elements misidentified in the global step (Table 6).

4. Extended Verification

The transverse displacements at nodes along or near the edges of the plate are quite trivial, so damages that occur in these positions affect mode shape change inconsiderably. Additionally, multiple damages may also appear simultaneously on the plate with different damage ratios. Therefore, it is a pretty difficult task to identify the damages near the boundaries and detect the multidamages. To evaluate the applicability and the accuracy of the global and local MSE-based damage localization procedure, a 360×240 mm rectangular aluminum plate with two surface cracks with size 36×2.4 mm is considered. The stiffness degradation of the cracks is assumed to be 10%. Figure 12 depicts the location of two cracks, one at the long edge and one in the midspan of the plate. The material aluminum properties are the same as the previous problem: Elastic modulus E = 70 GPa, Poisson coefficient υ = 0.33, and mass density ρ = 2735 kg/m3. In this case, four edges of the plate are fixed to consider the effect of small modal amplitude at the boundaries to the diagnosed results.

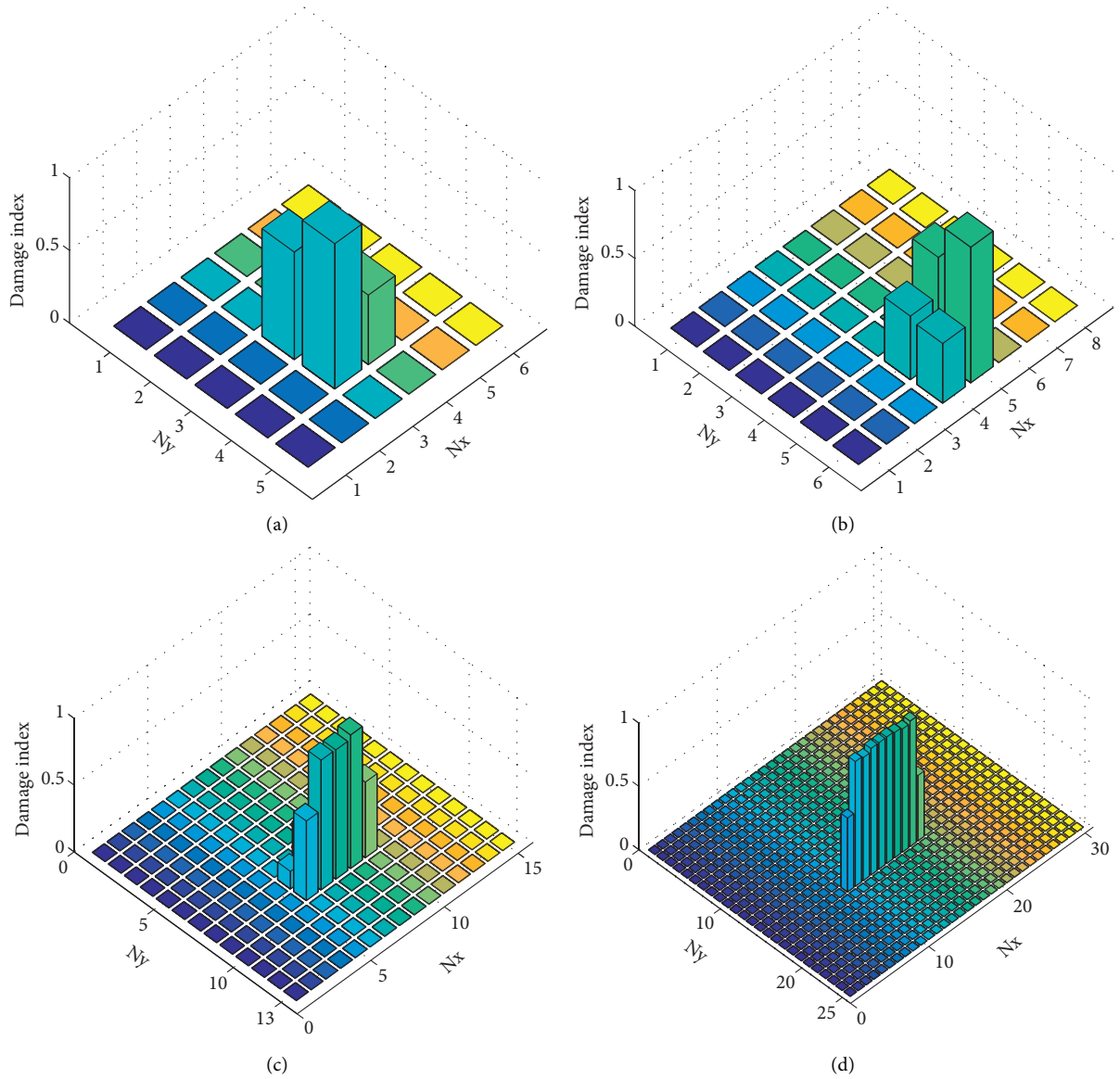

Figure 17: Truncated damage index charts of the second preliminary damaged area using damage threshold 40% $Z_{ij}^{\max}$: (a) Mesh 5%, (b) Mesh 4%, (c) Mesh 2%, and (d) Mesh 1%.

Table 8: Damage capacity indicators for the first preliminary damaged area.

Mesh size	Indicator	Damage threshold					
		20%	30%	40%	50%	60%	70%
5%	A (%)	100	67	67	67	67	33
	B (%)	1150	933	683	683	683	217
4%	A (%)	100	100	100	67	67	67
	B (%)	700	700	540	253	253	253
2%	A (%)	100	100	100	100	100	80
	B (%)	300	300	300	220	180	80
1%	A (%)	100	100	100	100	100	90
	B (%)	200	110	0	0	0	0

The global and local procedures are deployed sequentially to identify the location of cracks. Figure 13 shows the first three flexural mode shapes of the undamaged plate with fixed boundary conditions. Figure 14 presents the truncated damage index charts acquired from the global procedure, using three mesh sizes of 20%, 10%, and 5%. The charts show

Table 9: Damage capacity indicators for the second preliminary damaged area.

Mesh size	Indicator	Damage threshold					
		20%	30%	40%	50%	60%	70%
5%	A (%)	100	100	67	67	67	33
	B (%)	1400	1400	933	933	683	467
4%	A (%)	100	100	67	67	67	33
	B (%)	860	860	573	573	573	287
2%	A (%)	100	100	100	100	100	100
	B (%)	380	300	300	220	220	100
1%	A (%)	100	100	100	100	100	100
	B (%)	200	70	0	0	0	0

that the global procedure can identify the occurrence of two cracks even with the large mesh sizes (Table 7). As shown in Figure 15, two preliminary damaged areas are separated from the whole plate to apply the local procedure.

Figure 16 and Figure 17 show the damage index charts of two preliminary damaged areas obtained from the local MSE procedure using different mesh sizes of 5%, 4%, 2%, and 1%, respectively. The damage detection results using local procedure are displayed in Table 8 and Table 9. It is noted that indicator B of the 1% mesh size is the best for both damage locations and all of the used damage thresholds. In terms of damage thresholds, indicator B of the 1% mesh size reaches a minimum of 0% from the damage threshold of 40%.

5. Conclusion

In this paper, the MSE-based damage localization method is developed successfully to detect structural damages in plates. Three remarkable conclusions are obtained from the analyzed damage scenarios:

(1) The two-step procedure accurately detects damages in plates considering various boundary conditions. First, the global MSE was deployed on the whole plate using the mesh size of 5% plate dimension to locate the preliminary damaged areas. Second, the local MSE was then applied to these areas to precisely determine the size of damages using the mesh size of 1% plate dimension mesh size.

(2) The local MSE is not dependent on boundary conditions of the total plate and the transverse displacement data at the nodes outside the preliminary damaged area. These are the superior advantages of the two-step MSE-based damage detection procedure. As a result, the local approach uses much less modal data and gives better damage identification accuracy than the global one.

(3) The proposed MSE-based damage localization procedure can detect precisely the location and the size of the cracks for many different positions. The procedure using the combination of three first mode shapes and a threshold of 40% gives the best results of damage localization. In addition, the proposed procedure is capable of accurately detecting both damaged and undamaged areas.

Data Availability

The data used to support the findings of this study are included within the article.

Conflicts of Interest

The authors declare that there are no conflicts of interest regarding the publication of this paper.

Acknowledgments

This research is funded by Vietnam National University Ho Chi Minh City (VNU-HCM) under grant number B2020-20-06. We acknowledge the support of time and facilities from Ho Chi Minh City University of Technology (HCMUT), VNU-HCM for this study.

References

[1] M. Yang, H. Zhong, M. Telste, and S. Gajan, "Bridge damage localization through modified curvature method," *Journal of Civil Structural Health Monitoring*, vol. 6, no. 1, pp. 175–188, 2015.

[2] H. Zhong and M. Yang, "Damage detection for plate-like structures using generalized curvature mode shape method," *Journal of Civil Structural Health Monitoring*, vol. 6, no. 1, pp. 141–152, 2015.

[3] Z. Y. Shi, S. S. Law, and L. M. Zhang, "Structural damage localization from modal strain energy change," *Journal of Sound and Vibration*, vol. 218, no. 5, pp. 825–844, 1998.

[4] A. Alvandi and C. Cremona, "Assessment of vibration-based damage identification techniques," *Journal of Sound and Vibration*, vol. 292, no. 1-2, pp. 179–202, 2006.

[5] N. Stubbs, J. T. Kim, and C. R. Farrar, "Field verification of a non-destructive damage localization and severity estimation algorithm," in *Proceedings of the 1995 13th International Modal Analysis Conference*, pp. 210–218, Nashville, TN, USA, February 1995.

[6] P. Cornwell, S. W. Doebling, and C. R. Farrar, "Application of the strain energy damage detection method to plate-like structures," *Journal of Sound and Vibration*, vol. 224, no. 2, pp. 359–374, 1999.

[7] H. W. Shih, D. P. Thambiratnam, and T. H. T. Chan, "Vibration based structural damage detection in flexural members using multi-criteria approach," *Journal of Sound and Vibration*, vol. 323, no. 3-5, pp. 645–661, 2009.

[8] T.-C. Le, D.-D. Ho, T.-C. Huynh, and V.-S. Bach, "Crack detection in plate-like structures using modal strain energy

method considering various boundary conditions," *Shock and Vibration*, vol. 2021, pp. 1–17, Article ID 9963135, 2021.

[9] S. M. Seyedpoor, "A two stage method for structural damage detection using a modal strain energy based index and particle swarm optimization," *International Journal of Non-linear Mechanics*, vol. 47, no. 1, pp. 1–8, 2012.

[10] Y.-J. Cha and O. Buyukozturk, "Structural damage detection using modal strain energy and hybrid multiobjective optimization," *Computer-Aided Civil and Infrastructure Engineering*, vol. 30, no. 5, pp. 347–358, 2015.

[11] T. Vo-Duy, V. Ho-Huu, H. Dang-Trung, and T. Nguyen-Thoi, "A two-step approach for damage detection in laminated composite structures using modal strain energy method and an improved differential evolution algorithm," *Composite Structures*, vol. 147, pp. 42–53, 2016.

[12] P. Torkzadeh, H. Fathnejat, and R. Ghiasi, "Damage detection of plate-like structures using intelligent surrogate model," *Smart Structures and Systems*, vol. 18, no. 6, pp. 1233–1250, 2016.

[13] A. Kaveh and A. Zolghadr, "Cyclical parthenogenesis algorithm for guided modal strain energy based structural damage detection," *Applied Soft Computing*, vol. 57, pp. 250–264, 2017.

[14] D. Dinh-Cong, T. Vo-Duy, V. Ho-Huu, and T. Nguyen-Thoi, "Damage assessment in plate-like structures using a two-stage method based on modal strain energy change and JAYA algorithm," *Inverse Problems in Science and Engineering*, vol. 27, no. 2, pp. 166–189, 2018.

[15] S. Khatir, M. Abdel Wahab, D. Boutchicha, and T. Khatir, "Structural health monitoring using modal strain energy damage indicator coupled with teaching-learning-based optimization algorithm and isogoemetric analysis," *Journal of Sound and Vibration*, vol. 448, pp. 230–246, 2019.

[16] J. Zhao, M. Shi, G. Yin, and X. Lian, "Damage localization based on modal strain energy index and evidence theory," *E3S Web of Conferences*, vol. 165, Article ID 06053, 2020.

[17] H. Fathnejat and B. Ahmadi-Nedushan, "An efficient two-stage approach for structural damage detection using meta-heuristic algorithms and group method of data handling surrogate model," *Frontiers of Structural and Civil Engineering*, vol. 14, no. 4, pp. 907–929, 2020.

[18] H. Nick, A. Aziminejad, M. Hamid Hosseini, and K. Laknejadi, "Damage identification in steel girder bridges using modal strain energy-based damage index method and Artificial Neural Network," *Engineering Failure Analysis*, vol. 119, Article ID 105010, 2021.

[19] A. Kaveh, P. Rahmani, and A. Dadras Eslamlou, "Damage Detection Using a Graph-Based Adaptive Threshold for Modal Strain Energy and Improved Water Strider Algorithm," *Periodica Polytechnica Civil Engineering*, vol. 65, 2021.

[20] Q. Fan, "A two-step damage identification based on cross-model modal strain energy and simultaneous optimization," *IOP Conference Series: Earth and Environmental Science*, vol. 643, no. 1, Article ID 012145, 2021.

[21] F. Sadeghi, Y. Yu, X. Zhu, and J. Li, "Damage identification of steel-concrete composite beams based on modal strain energy changes through general regression neural network," *Engineering Structures*, vol. 244, Article ID 112824, 2021.

[22] K. Belhadj, N. B. Guedria, A. Helali, and C. Bouraoui, "A two-stage approach to solve structural damage detection problem in plate structures," *Lecture Notes in Mechanical Engineering*, pp. 63–72, 2021.

[23] H.-W. Hu and C.-B. Wu, "Nondestructive damage detection of two dimensional plate structures using modal strain energy method," *Journal of Mechanics*, vol. 24, no. 4, pp. 319–332, 2008.

[24] R. D. Blevins, *Formulas for Natural Frequency and Mode Shape*, Krieger Publishing Company, Malabar, Florida, 2001.